2020-06

Diffusion tensor imaging of lumbar spinal nerves reveals changes in microstructural integrity following decompression surgery associated with improvements in clinical symptoms: A case report

Hughes, SW

10.1016/j.mri.2020.02.007
Magnetic Resonance Imaging
Elsevier BV

Diffusion tensor imaging of lumbar spinal nerves reveals changes in microstructural integrity following decompression surgery associated with improvements in clinical symptoms: A case report

Hughes SW[1*], Hellyer PJ[2,3], Sharp DJ[2], Newbould RD[4], Patel MC[5], Strutton PH[1]

[1] The Nick Davey Laboratory, Division of Surgery, Imperial College London, UK.

[2] Computational, Cognitive and Clinical Neuroimaging Laboratory, Division of Brain Sciences, Imperial College London, London, UK.

[3]Department of Bioengineering, Imperial College London, UK.

[4]Imanova, Ltd, UK.

[5]Imaging Department, Imperial College Healthcare NHS Trust, Charing Cross Hospital, London, UK.

[*]Corresponding author Address: The Nick Davey Laboratory, Human Performance Group, Division of Surgery, Department of Surgery and Cancer, Faculty of Medicine, Imperial College London, W6 8RF. Tel: +44 (0)20 331 38837; fax: +44 (0)20 331 38835. Email: sam.hughes@imperial.ac.uk

Abstract

The outcomes from spinal nerve decompression surgery are highly variable with a sizable proportion of elderly foraminal stenosis patients not regaining good pain relief. A better understanding of nerve root compression before and following decompression surgery and whether these changes are mirrored by improvements in symptoms may help to predict the likelihood of positive post-surgical outcomes. This study used a combination of diffusion tensor imaging (DTI), clinical questionnaires and motor neurophysiology assessments before and up to 3 months following spinal decompression surgery. In this case report, a 70-year-old women with compression of the left L5 spinal nerve root in the L5-S1 exit foramina was recruited to the study. At 3 months following surgery, DTI revealed marked improvements in left L5 microstructural integrity to a similar level to that seen in the intact right L5 nerve root. This was accompanied by a gradual improvement in pain-related symptoms, mood and disability score by 3 months. These results provide insight into the factors (e.g. microstructural damage to nerve roots) which may be able to predict positive outcomes following decompression surgery.

Key words: Diffusion tensor imaging; Surgery; Pain, Motor; Symptoms; Stenosis

1 Introduction

Foraminal stenosis often results in the compression of exiting spinal nerve roots and is associated with the development of severe functional impairment and radicular pain symptoms [1]. Age-related spinal degenerative changes in disc height, facet joints and ligamentum flavum are all common causes of spinal nerve root compression and decompression surgery is often performed in an attempt to resolve symptoms and restore function [2]. However, the outcome of surgery is highly variable with approximately 50 - 60% of patients reporting good to excellent results [3].

Currently, the primary diagnostic indicator for the surgical decision-making process is spinal MRI which is able to provide valuable information about the extent of stenosis and its compression of the adjacent spinal nerves [4, 5]. However, a potential factor not examined in as much detail so far is the microstructural integrity or damage to nerve fibres traversing the intervertebral foramen. Diffusion tensor imaging (DTI) and DTI with fibre tracking (i.e. tractography) has found clinical application in the evaluation of the central nervous system and has been extensively used to image white matter tracts [6, 7]. It would be therefore prudent to explore our novel imaging and data processing methods [8, 9], currently used in other areas of neurology, to examine the degree of damage or compression to the nerves which are in the target area of the surgical procedures.

We have previously shown that DTI can be used to measure the microstructural integrity along spinal nerve roots in healthy volunteers and elderly foraminal stenosis patients, which correlate with motor function tested neurophysiologically [8, 9]. Using DTI, it is possible to calculate fractional anisotropy (FA), mean diffusivity (MD), axial diffusivity (AD) and radial diffusivity (RD), which are sensitive to changes in microstructural integrity in injured nerves [10-12]. Pathological changes in diffusion metrics derived along compressed nerve roots have shown there to be reduction in FA values which provides a means by which to quantify nerve damage and provide insight into the underlying pathology [13-15]. Previous case report studies have shown the clinical application of using DTI to evaluate the degree of compression and to diagnose a symptomatic lesion caused by compression of the spinal nerves at the foramina [16, 17]. Further, we have shown that metrics derived from DTI correspond to clinical symptoms and the functional integrity of motor pathways in patients with foraminal stenosis [9]. What is not known, however, is whether improvements in function and patient-reported symptoms are associated with similar improvements in spinal nerve integrity following decompression surgery.

1.1 Case Presentation

Here we report a case of foraminal stenosis and left L5 nerve root compression found in a 70-year old female due to undergo lumbar decompression surgery. She is a retired nurse and has been having back problems with radiological symptoms for the past 3 years. With written and informed consent, the participant was recruited in July 2016 from a surgical waiting list at Imperial College NHS Trust and underwent a series of clinical questionnaires, DTI and neurophysiological assessments pre-surgery which were repeated following decompression surgery. Before the surgery, she felt as though her condition was rapidly deteriorating. Initial radiological assessments revealed that the lower three lumbar intervertebral discs were degenerate and all showed loss of disc space height. The thecal sac was in normal limits throughout the lumbar canal and the lower cord and conus were normal. At L5-S1 on the left as a result of a disc bulge, loss of disc height and facet joint hypertrophy, there was an impingement of the exiting L5 nerve root (figure 1A). Postoperatively, radiological findings showed there to be an improvement in the degree of nerve root compression in the L5-S1 exit foramen and she reported that her condition improved rapidly during the 3 months post-surgery with an almost complete resolution of her symptoms.

2 Methods

2.1 Imaging protocols

All MRI data were collected using a 3T Siemens Verio clinical MRI scanner (Siemens Healthcare, Erlangen Germany). The patient was imaged supine using an 11cm local loop coil centred over the intervertebral disc between L5 and S1 in combination with 2 elements of the phased-array spine coil to maximise the signal-to-noise ratio in the lumbar roots. Coil positioning was verified by initial localizer scans. Structural imaging for the radiological review by a consultant radiologist (author MP) to confirm evidence of lumbar nerve compression included sagittal T1-weighted (T1w) and T2-weighted (T2w) turbo spin echo (TSE), coronal T2w TSE, as well as a multislab T2w TSE angled axial to L3-L4, L4-L5 and L5-S1 vertebral discs. Diffusion weighted images (DWI) were acquired with b=800 s/mm^2 using a twice-refocused diffusion preparation, an inverted slice select gradient on the refocusing pulses for improved fat saturation [18], and a 2D EPI readout. 2.5 mm thick adjacent slices of a 100 x 256 mm field of view (FOV) were collected with TE=92 ms, TR=9 s, 50 x 128 resolution with readout bandwidth of 1562 Hz per pixel, giving a resolution of 2.0 x 2.0 x 2.5 mm. Saturation bands were placed superiorly and inferiorly to imaging slab to reduce flow and off-resonance excitation artefacts. 64 non-collinear directions interspersed with a b=0 measurement after every 16 directions were collected resulting in 68 acquisitions in 10m:21s [8, 9].

2.2 Questionnaires

The participant completed questionnaires during the pre-operative assessments and again at 1 month, 2 months and 3 months post-operatively. These questionnaire included an initial self-assessment which included duration of leg pain, type of pain (i.e. aching, shooting, stabbing), visual analogue scales for 'typical' and 'worse' pain (VAS; 0 – no pain, 10 – maximum pain). Hospital Anxiety and Depression Scale (HADS; 0 – no anxiety/depression, 21 – maximum anxiety/depression) and Oswestry Low Back Disability Questionnaire (ODI; 0, no disability; 100, maximum disability) and the Roland Morris Disability Questionnaire (RMDQ; 0, no disability; 24 maximum disability) were also completed.

2.3 Neurophysiology protocols

2.3.1 Recording. Electromyographic (EMG) recordings were obtained bilaterally from the tibialis anterior (TA). Pairs of Ag/AgCl electrodes (self-adhesive, 2 cm diameter, CareFusion, UK) were positioned parallel to the muscle fibre orientation. A ground electrode was placed over the left lateral malleolus. The electrodes were positioned at 1/3 way along a line between the head of the fibula and the superior aspect of the medial malleolus. The Participant was additionally asked to contract their TA muscle by ankle dorsiflexion to confirm that the electrodes were located on the most prominent muscle bulk. EMG data were filtered (10–1000 Hz), amplified (1000×; Iso-DAM, World Precision Instruments, UK) and sampled at 2 kHz using a Power 1401 data acquisition system and Signal v5 software (Cambridge Electronic Design [CED], UK) connected to a computer for subsequent offline analysis.

2.3.2 Transcranial magnetic stimulation (TMS). TMS was delivered to the motor cortex using a Magstim 200^2 mono-phasic stimulator (The Magstim Company Ltd., UK) connected to a figure-of-eight coil (wing outer diameter 10 cm), positioned over the approximate location of primary motor cortex at a site which elicited a maximal motor evoked potential (MEP) in the contralateral target muscle.

2.3.3 Experimental parameters. Measurements were conducted while the participant was seated in an armchair with torso supported by a backrest and feet strapped securely on a wood plate on the floor. Three brief (~2s) maximum voluntary contractions (MVC), with at least 10s rest between contractions, were recorded from each TA muscle; strong verbal encouragement was provided throughout. The mean rectified EMG over 500ms during each of the three MVCs was calculated and averaged and 10% of this value was displayed continuously on a screen as visual feedback for the participant during all TMS measurements.

2.3.4 Corticospinal excitability. Measurements were performed on each TA muscle separately while the participant maintained contraction levels at 10% MVC. Active motor threshold (AMT) was

established for each TA muscle, which was defined as the lowest intensity of TMS that evoked visible MEPs in at least three of six consecutive trials. Motor evoked potentials (MEPs) were evoked by TMS and the maximal MEP amplitude (MEP_{max}) was determined by increasing stimulus intensities in 10% steps of the AMT until the MEP amplitude did not show additional increases or the intensity reached to the maximal device output. Six MEPs were recorded; TMS pulses were given every 8 s with several periods of rest given to the participant between trials to avoid muscle fatigue.

2.3.5 M-wave and F-waves. A maximal motor response (M_{max}) and F-waves were measured following supramaximal stimuli via a cathode to the common peroneal nerve around the fibular head (Digitimer DS7, Digitimer UK, 500-μs pulse duration). The anode was placed over the patella on the stimulated side. Five M_{max} at the same intensity were recorded; an intensity of 120% of the intensity used to elicit M-max was delivered to the nerve at 1Hz until 20 F-waves were recorded.

2.4 Data analysis

2.4.1 DTI. The post-processing of diffusion-weighted images (DWI) and fitting of the diffusion tensor were performed using the FSL Diffusion Toolbox (FDT) (FSL, http://fsl.fmrib.ox.ac.uk/fsl) v.5.0.6 (Oxford, UK). From the estimation of the diffusion tensor at each individual voxel, voxel-wise measures of Fractional Anisotropy (FA) were derived along affected and unaffected nerves. Regions of Interest (ROIs) were manually drawn with reference to the axial view of b=0 image from the diffusion acquisition overlaid onto the co-acquired Axial T2-weighted image (see Figure 1). Three binary ROIs were manually traced onto the image using FSLview (FSL, http://fsl.fmrib.ox.ac.uk/fsl) on both the affected and unaffected L5 nerves below the disc in the foraminal zone (i.e. ~12mm distal to the centre of the L4-L5 disc). Each ROI was drawn to cover the entire visible signal on the b=0 image which was clearly differentiable as nerve, resulting in ROIs of between 40 and 60-mm^3. This size of ROI reduces the partial volume effect; the cross-sectional area of nerve roots in the lower lumbar region has been shown in a cadaveric study to be 34.48 ± 11.25mm^2 [19].

2.4.2 Tractography. For visualisation, basic fibre tracking analysis was performed at the level of each of the L5 spinal nerves. Fibre orientation distribution (FOD) analysis and fibre tracking was performed on the DWI data using MRtrix (https://github.com/MRtrix3/mrtrix3). Voxelwise FODs were estimated using constrained spherical deconvolution, with an lmax of 6. Probabilistic tractography was performed the iFOD2 algorithm [20], with a step size of half the DWI voxel-size, a turning angle threshold of 90° and a streamline termination threshold of FOD<0.1. Tracks were seeded from the spinal canal superior to the L5 nerves, and terminated on entering the most distal ROI in each of the bilateral L5 nerves. Streamlines were seeded at random from the seed until maximum streamlines successfully traversed from the seed to each of the target ROIs.

2.4.3 Neurophysiology. The mean MEP amplitude per stimulus intensity was calculated and normalised to the M-max for each muscle; this was defined as MEPmax. Mean pre-stimulus EMG was calculated in a 100-ms window from the rectified EMG traces for the TA and soleus at each intensity. The average rectified EMG trace from the trials in which 120% AMT was delivered was used to derive the MEP latency for each muscle. The amplitude and latency of averaged M_{max} were measured and the minimum latency of F waves was identified from the recorded 20 F waves. The F wave persistence was calculated as the number of F waves obtained per the number of stimulations. Peripheral motor conduction time (PMCT) was calculated using the following equation:

$$\text{PMCT (ms)} = \frac{\text{Mmax latency } + \text{minimum F wave latency} - 1}{2}$$

3 Results

3.1 Decompression surgery was associated with an improvement in spinal nerve microstructural integrity

Post-operative radiological findings showed there to be a mild improvement in the degree of stenosis at the L5-S1 exit foramen (Figure 1A right). However, tractography analysis showed that there was a noticeable increase in the density of streamlines in the left L5 nerve root following decompression surgery (Figure 1B right and Table 1). Further, comparison of pre- and post-operative DTI assessments showed that there was a lower FA in the affected L5 nerve root within the exit foramen which had increased to a similar level to that measured from the intact right L5 nerve root following surgery (Table 1).

3.2 Temporal changes in pain symptoms and co-morbidities by 3 months following decompression surgery

3.2.1 Pre-op: During the pre-operative assessment, the patient reported having problems carrying out most daily activities, with a shooting leg pain rated as 5/10 which was present most of the time and was exacerbated when she starting walking (Table 2). She reported co-morbid changes in her mental health, scoring 15 on the HADS index for both anxiety and depression. The nerve compression was also associated with moderate to severe levels of overall disability (ODI: 48; RMDQ: 12).

3.2.2 1 month post-op: The patient could manage most of her daily tasks and could walk approximately ½ mile before a sharp pain started. However, she still reported pain most of the time which she rated as 5/10. Her levels of anxiety and depression had both reduced to 4 on the HADS index. However, her overall disability level had not improved (ODI: 56, RMDQ: 14).

3.3.3 2 months post op: The patient reported that she had started to develop problems with some of her daily activities and that an aching pain rated as 6/10 was present most of the time which would be exacerbated by walking over 100 yards. There was an improvement in both anxiety and depression scores (anxiety: 2; depression, 2), however the overall level of disability was still moderate to severe (ODI: 44; RMDQ: 12).

3.3.4 3 months post-op: The patient reported that she could manage all of her daily activities and that she occasionally experiences an aching leg pain which was rated as 1/10, however this was still exacerbated by walking over 100 yards. Her anxiety and depression HADS scores remain low (anxiety: 3; depression: 2) and her overall levels of disability had reduced (ODI: 31; RMDQ: 10).

3.3 Improved integrity in motor pathways following decompression surgery

The integrity of peripheral and central motor pathways were assessed pre-operatively and again at 3 months following decompression surgery. The maximum normalised MEP amplitude evoked from the affected TA muscle during the pre-operative phase was approximately 50% lower than the post-operative response measured at 3 months (Table 3) which had increased to a similar level to the motor responses observed in the contralateral limb. This was mirrored by an increase in the MEP area, peripheral motor conduction time and F-wave persistence following decompression surgery.

4 Discussion

In this case report, we have shown that DTI can be used to track improvements in the microstructural integrity of compressed spinal nerve roots following decompression surgery in an elderly foraminal stenosis patient. Critically, we show that these changes are accompanied by improvements in pain symptoms as well as overall levels of disability and the integrity of both central and peripheral motor pathways. When used in combination with MRI, these advanced diffusion weighted imaging protocols could give further insight into the underlying microstructrual changes in compressed nerve roots, which give rise to specific symptoms and functional impairments. This may help to better understand individual responses to surgery and may affect surgical decision-making processes.

There is a growing body of evidence which suggest that DTI and the use of spinal nerve tractography can be used to quantify and visualise nerve root compression [13-15, 17, 21]. Here, we shown that in an elderly 70 year old patient diagnosed with foraminal stenosis, there was a reduction in FA and a reduced track density in the compressed nerve root, which increased to a level similar to that seen in the right intact nerve root following surgery. This is in line with previous larger cohort studies, which have shown a pathological drop in FA values along compressed nerve roots [9, 14, 21] as well as abnormalities in tractography as the nerves pass through the foramen [22]. The results from a

previous case report suggest that DTI provides a significant advantage over the use of conventional imaging in the diagnosis of foraminal stenosis by reducing the occurrence of false-positives which are often associated with the use of MRI [16]. Critically, our data also provides further insight into the sensitivity of diffusion metrics to change following surgical intervention as we found an increase in FA and track density following decompression surgery in this patient.

FA provides a detailed summary of water diffusion along nerve roots and changes are thought to be linked with nerve injury-induced Wallerian degeneration and subsequent changes in microstructural integrity [23, 24]. Detailed morphological studies in animals have shown that spinal nerve decompression is associated with an increase in the number of myelinated axons [25] and it is possible that the increase in FA value measured 3 months following surgery is due to regenerative changes in the nerve root microstructural integrity [26]. It is therefore likely that diffusion metrics not only provide an indication of the presence of a neuropathy, but also provides insight into the underlying pathological changes that may be reversed following decompression surgery [27]. This patient with a 3-year history of low back pain with radicular symptoms had an improvement in nerve root integrity and function following decompression surgery. It is possible that longer duration of symptoms may be associated with a reduced chance of nerve root regeneration and resolution of symptoms following decompression [28]. Equally, the severity of nerve root compromise may serve as another predictive factor for surgical success and it is feasible that DTI can be used to reveal the extent of nerve compression and help guide the clinical decision making process.

As well as improvements in nerve root microstructural integrity, the patient also reported gradual improvements in pain related symptoms and overall levels of disability during the 3 months following surgery. This is in line with the results of a large prospective study carried out at our institution, where decompression surgery was associated with gradual improvements in clinical symptoms by 6 weeks [3, 29]. We have previously shown that diffusion metrics derived from compressed nerve roots correlate with pain severity as well as depression scores [9]. Interestingly, this case report provides the first evidence of an improvement in both clinical symptoms and the integrity of a decompressed nerve root.

We have previously shown that in healthy volunteers and elderly foraminal stenosis patients that DTI metrics derived spinal nerve roots correlate with a number of motor neurophysiological tests [8, 9]. The results derived from this patient show relatively severe motor deficiencies during the pre-operative assessment which had dramatically improved by 3 months following decompression surgery. This is line with the patient's improvement in overall levels of disability as well as a previous animal study which demonstrated that DTI parameters correlate with the degree of motor and sensory

recovery following successful release of the nerve entrapment [33]. Damage to nerve roots is associated with focal damage to myelin sheath which is reflected in a slowing of nerve conduction velocity [34, 35]. In this case report, we show improvements in peripheral motor conduction time following decompression surgery suggesting regeneration of nerve root function which was also reflected in the improvements in microstructural integrity assessed by DTI. It is possible that FA not only provides insight into the degree of nerve compression but may also be an indication of demyelination at the site of compression.

5 Conclusion

This study provides evidence that DTI can be used to monitor changes in the degree of nerve root compression which is mirrored by improvements in pain-related symptoms. DTI may therefore provide an advantage over conventional diagnostics tools, such as nerve conduction studies and conventional MRI, which often correlate poorly with patient reported symptoms [30, 31]. By showing concurrent improvements in nerve root integrity and pain-related symptoms in this patient, the current study provides the rationale to carry out detailed investigations into the relationship between the extent of nerve compression, its function and the development of pain and disability-related symptoms before and after surgery.

Declarations of Interest

None

Funding

This work was supported by Dunhill Medical Trust (grant number R401/0215).

Figure legends

Figure 1. Changes in left L5 nerve root compression following decompression surgery. A) Left: sagittal T2 weighted MRI showing left L5 nerve root compression in the exit foramen; right: MRI findings 3 months following decompression surgery. B) Left: Coronal T2 weighted MRI with tractography overlaid showing the compressed left L5 nerve; right: Improvements in the left L5 tract density 3 months following decompression.

Table legends

Table 1. Fractional anisotropy and tract density (streamlines) derived from the compressed and intact L5 nerve root before and after decompression surgery.

Table 2. Patient-reported changes in mood, disability and leg pain and pain-related symptoms following decompression surgery. Descriptions of symptoms pre-surgery and at 1, 2 and 3 months following surgery. HADS, hospital anxiety and depression index; ODI, Oswestry Disability Index; NRS, numerical rating scale.

Table 3. Changes in peripheral and central motor pathways of the affected limb following decompression surgery. Values show changes in neurophysiological assessments 3 months following surgery. MEP, motor evoked potential; PMCT, peripheral motor conduction time.

References

1. Genevay, S. and S.J. Atlas, *Lumbar spinal stenosis.* Best Pract Res Clin Rheumatol, 2010. **24**(2): p. 253-65.
2. McGregor, A.H., et al., *Rehabilitation following surgery for lumbar spinal stenosis.* Cochrane Database Syst Rev, 2013(12): p. CD009644.
3. McGregor, A.H. and S.P. Hughes, *The evaluation of the surgical management of nerve root compression in patients with low back pain: Part 1: the assessment of outcome.* Spine (Phila Pa 1976), 2002. **27**(13): p. 1465-70.
4. Geisser, M.E., et al., *Spinal canal size and clinical symptoms among persons diagnosed with lumbar spinal stenosis.* Clin J Pain, 2007. **23**(9): p. 780-5.
5. Jonsson, B., et al., *A prospective and consecutive study of surgically treated lumbar spinal stenosis. Part I: Clinical features related to radiographic findings.* Spine (Phila Pa 1976), 1997. **22**(24): p. 2932-7.
6. Hellyer, P.J., et al., *Individual prediction of white matter injury following traumatic brain injury.* Ann Neurol, 2013. **73**(4): p. 489-99.
7. Sharp, D.J., G. Scott, and R. Leech, *Network dysfunction after traumatic brain injury.* Nat Rev Neurol, 2014. **10**(3): p. 156-66.
8. Chiou, S.Y., et al., *Relationships between the integrity and function of lumbar nerve roots as assessed by diffusion tensor imaging and neurophysiology.* Neuroradiology, 2017.
9. Hughes, S.W., et al., *Diffusion tensor imaging reveals changes in microstructural integrity along compressed nerve roots that correlate with chronic pain symptoms and motor deficiencies in elderly stenosis patients.* Neuroimage Clin, 2019. **23**: p. 101880.
10. Takahashi, N., et al., *Pathomechanisms of nerve root injury caused by disc herniation: an experimental study of mechanical compression and chemical irritation.* Spine (Phila Pa 1976), 2003. **28**(5): p. 435-41.
11. Rydevik, B.L., et al., *Effects of acute, graded compression on spinal nerve root function and structure. An experimental study of the pig cauda equina.* Spine (Phila Pa 1976), 1991. **16**(5): p. 487-93.
12. Rydevik, B., M.D. Brown, and G. Lundborg, *Pathoanatomy and pathophysiology of nerve root compression.* Spine (Phila Pa 1976), 1984. **9**(1): p. 7-15.
13. Balbi, V., et al., *Tractography of lumbar nerve roots: initial results.* Eur Radiol, 2011. **21**(6): p. 1153-9.
14. Eguchi, Y., et al., *Discrimination between Lumbar Intraspinal Stenosis and Foraminal Stenosis using Diffusion Tensor Imaging Parameters: Preliminary Results.* Asian Spine J, 2016. **10**(2): p. 327-34.
15. Eguchi, Y., et al., *Clinical applications of diffusion magnetic resonance imaging of the lumbar foraminal nerve root entrapment.* Eur Spine J, 2010. **19**(11): p. 1874-82.

16. Eguchi, Y., et al., *Diagnosis of Lumbar Foraminal Stenosis using Diffusion Tensor Imaging.* Asian Spine J, 2016. **10**(1): p. 164-9.
17. Kitamura, M., et al., *A case of symptomatic extra-foraminal lumbosacral stenosis ("far-out syndrome") diagnosed by diffusion tensor imaging.* Spine (Phila Pa 1976), 2012. **37**(14): p. E854-7.
18. Nagy, Z. and N. Weiskopf, *Efficient fat suppression by slice-selection gradient reversal in twice-refocused diffusion encoding.* Magn Reson Med, 2008. **60**(5): p. 1256-60.
19. Inufusa, A., et al., *Anatomic changes of the spinal canal and intervertebral foramen associated with flexion-extension movement.* Spine (Phila Pa 1976), 1996. **21**(21): p. 2412-20.
20. Brefel-Courbon, C., et al., *Clinical and imaging evidence of zolpidem effect in hypoxic encephalopathy.* Ann Neurol, 2007. **62**(1): p. 102-5.
21. Orita, S., et al., *Lumbar foraminal stenosis, the hidden stenosis including at L5/S1.* Eur J Orthop Surg Traumatol, 2016. **26**(7): p. 685-93.
22. Eguchi, Y., et al., *Quantitative evaluation and visualization of lumbar foraminal nerve root entrapment by using diffusion tensor imaging: preliminary results.* AJNR Am J Neuroradiol, 2011. **32**(10): p. 1824-9.
23. Beaulieu, C. and P.S. Allen, *An in vitro evaluation of the effects of local magnetic-susceptibility-induced gradients on anisotropic water diffusion in nerve.* Magn Reson Med, 1996. **36**(1): p. 39-44.
24. O'Donnell, L.J. and C.F. Westin, *An introduction to diffusion tensor image analysis.* Neurosurg Clin N Am, 2011. **22**(2): p. 185-96, viii.
25. Jancalek, R. and P. Dubovy, *An experimental animal model of spinal root compression syndrome: an analysis of morphological changes of myelinated axons during compression radiculopathy and after decompression.* Exp Brain Res, 2007. **179**(1): p. 111-9.
26. Pham, K. and R. Gupta, *Understanding the mechanisms of entrapment neuropathies. Review article.* Neurosurg Focus, 2009. **26**(2): p. E7.
27. Jung, J., et al., *Early Surgical Decompression Restores Neurovascular Blood Flow and Ischemic Parameters in an in Vivo Animal Model of Nerve Compression Injury.* J Bone Joint Surg Am, 2014. **96**(11): p. 897-906.
28. Chandra, P.S., et al., *Early versus delayed endoscopic surgery for carpal tunnel syndrome: prospective randomized study.* World Neurosurg, 2013. **79**(5-6): p. 767-72.
29. Anjarwalla, N.K., L.C. Brown, and A.H. McGregor, *The outcome of spinal decompression surgery 5 years on.* Eur Spine J, 2007. **16**(11): p. 1842-7.
30. Mondelli, M., et al., *Relationship between the self-administered Boston questionnaire and electrophysiological findings in follow-up of surgically-treated carpal tunnel syndrome.* J Hand Surg Br, 2000. **25**(2): p. 128-34.
31. Longstaff, L., et al., *Carpal tunnel syndrome: the correlation between outcome, symptoms and nerve conduction study findings.* J Hand Surg Br, 2001. **26**(5): p. 475-80.
32. Amundsen, T., et al., *Lumbar spinal stenosis. Clinical and radiologic features.* Spine (Phila Pa 1976), 1995. **20**(10): p. 1178-86.
33. Takagi, T., et al., *Visualization of peripheral nerve degeneration and regeneration: monitoring with diffusion tensor tractography.* Neuroimage, 2009. **44**(3): p. 884-92.
34. Kane, N.M. and A. Oware, *Nerve conduction and electromyography studies.* J Neurol, 2012. **259**(7): p. 1502-8.
35. Whittaker, R.G., *The fundamentals of electromyography.* Pract Neurol, 2012. **12**(3): p. 187-94.

Figure 1.

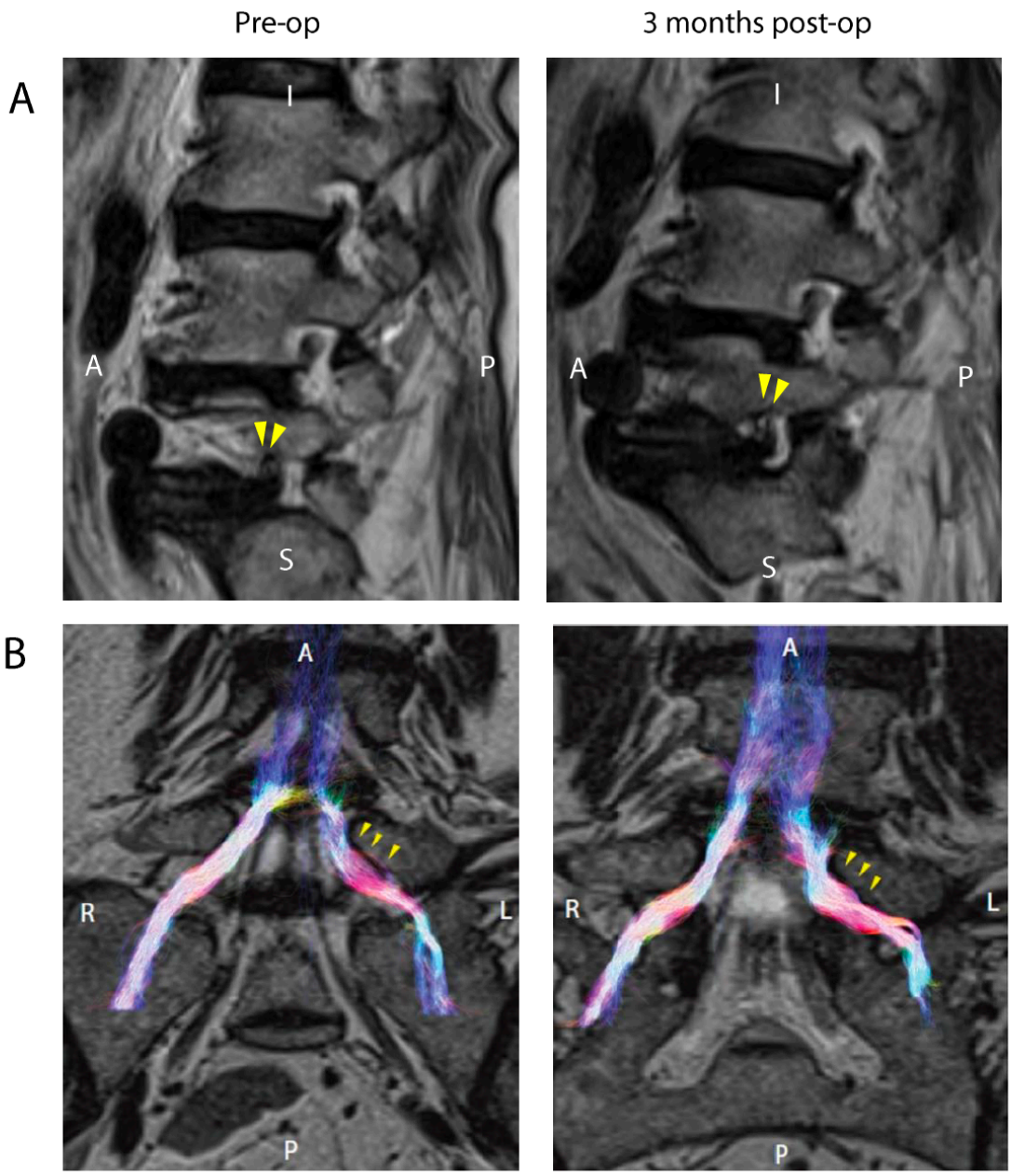

Table 1.

		Foraminal zone	
		Left (affected)	Right (unaffected)
FA	Pre-op	0.23	0.36
	Post-op	0.33	0.34
Streamlines	Pre-op	1558	2622
	Post-op	1799	2453

Table 2.

	Pre-op	1 month	2 month	3 month
HADS anxiety	15	4	2	3
HADS depression	15	4	2	2
Roland Morris	12	14	12	10
ODI	48	56	44	31
Leg Pain (NRS)	5	5	6	1
How do you think your back problem is progressing?	Rapidly getting worse	Gradually improving	Up and down	Gradually improving
How often do you experience leg pain?	Most of the time	Most of the time	Most of the time	Occasionally
How would you describe your leg pain?	Shooting	Sharp	Ache	Ache
Ability to cope with daily activities	I have problems with most daily activities	I can manage all my daily tasks	I have problems with some daily activities	I can manage all my daily tasks

Table 3.

MEP max (% M-wave max)	Pre-op	14.9
	Post-op	31.2
MEP area (mV.ms)	Pre-op	1.9
	Post-op	3.1
PMCT (ms)	Pre-op	19.1
	Post-op	15.0
F wave persistence (%)	Pre-op	31.4
	Post-op	64.5